Joint Pathology Center
Veterinary Pathology Services

WEDNESDAY SLIDE CONFERENCE 2024-2025

Conference #7 02 October 2024

CASE I:

Signalment:
8-year-old, male castrated, 20.3 kilograms crossbreed dog (*Canis lupus familiaris)*

History:
The dog was rescued by a local animal shelter and presented to Ross University Veterinary Clinic for panting. All vitals and hematologic and serum chemical analysis results were within the reference range. Two weeks later, the dog was presented again for evaluation of difficulty breathing, non-productive cough, and inappetence. On physical examination of the most recent consultation, the dog was depressed with a lowered head carriage and showed signs of dyspnea and abdominal breathing. Auscultation revealed muffled heart sounds. The veterinarian discussed the possibility of a late-stage tumor and suggested euthanasia if the condition deteriorated due to quality-of-life concerns. The patient presented again five days later with worsened respiratory distress and recurrence of pleural effusion. Euthanasia was elected.

Gross Pathology:
Abdominal ultrasonography revealed splenomegaly with abnormal echogenicity. Thoracic radiographs showed pleural effusion, loss of silhouette sign, and nodular interstitial pattern of the lungs. Thoracocentesis drained out approximately 1.15 litters of serosanguineous fluid from each side. On thoracic radiographs, after thoracocentesis, a persistent opacity was noted in the left caudal lung field. On skeleton radiographs, marked thickening and deformity of long bones with periosteal new bone formation was noted on distal bones of both front and hindlimbs, including the humerus, radius, carpus, tibia, ulna, metatarsal, and metacarpal bones.

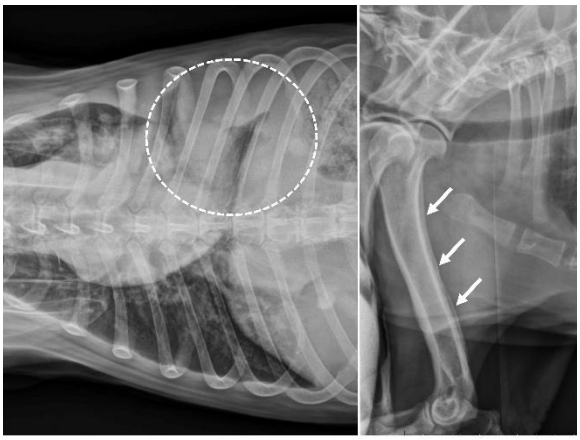

Figure 1-1. Survey radiographs, dog. Thoracic radiographs showed pleural effusion, loss of silhouette sign, and nodular interstitial pattern of the lungs. Thickening and deformity of long bones with periosteal new bone formation was noted on bones of the appendicular skeletal, including the humerus (arrows). (*Photo courtesy of:* Ross University School of Veterinary Medicine, St. Kitts, West Indies www.veterinary.rossu.edu).

On autopsy, approximately 90% of the left caudal lung lobe was infiltrated by a raised, moderately firm, irregularly shaped tan-white mass, 10-cm in largest diameter, with areas of hemorrhage, necrosis, and mucus on cross-sections. The rest of the lung lobes contained multifocal white raised nodules up to 1 cm in

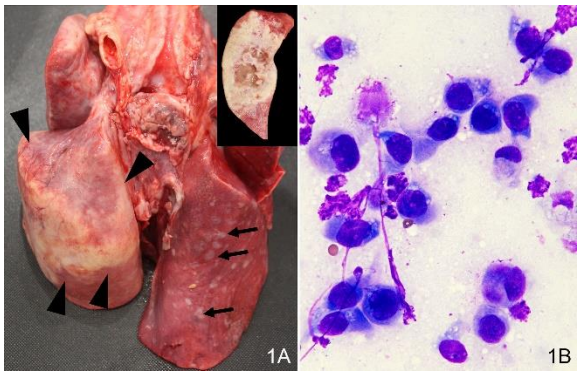

Figure 1-2. Lung, dog. A) Approximately 90% of the left caudal lung lobe is infiltrated by a raised, moderately firm, irregularly shaped tan-white mass, 10-cm in largest diameter. The rest of the lung lobes contained multifocal white raised nodules up to 1 cm in diameter. B) Cytologic demonstrates numerous pleomorphic polygonal cells admixed with fewer neutrophils. (*Photo courtesy of:* Ross University School of Veterinary Medicine, St. Kitts, West Indies, www.veterinary.rossu.edu).

diameter. The costal, mediastinal, and diaphragmatic pleura contained foci of white fibrotic plaques and adhesions to the pericardium. The pericardium was diffusely thickened with multiple coalescing white raised nodules. The distal esophagus near the cardia was thickened and had a 7-cm-diameter cystic lesion containing yellow viscous fluid. The spleen was attached to the omentum and contained a 2.5 cm round nodule near the attachment site. The caudal pole of the left kidney contained multiple raised grey to brown nodules extending to the renal cortex and appeared to be cystic on cross sections.

Laboratory Results:

In the past four months before the last consultation, serial hematologic and serum chemistry analysis during routine checkups showed a combination of mild mature neutrophilia (13.44 X 10^3 neutrophils/µL; reference interval, 3.00 X 10^3 to 12.00 X 10^3 neutrophils/µL), mild non-regenerative anemia, and mild hyperglobulinemia (5.6 g/dL; reference interval, 2.3 to 5.2 g/dL). On serologic qualitative test (Snap 4Dx Plus test, IDEXX laboratories Inc), the dog tested negative for heartworm disease, ehrlichiosis, Lyme disease, and anaplasmosis.

Table 1: Immunochemistry panel (lungs)

Marker	Results
Cytokeratin	80-90% positivity
Thyroid transcription factor 1	60-75% positivity
Napsin A	40% positivity

Microscopic Description:

Lungs: focally and extensively effacing the pulmonary parenchyma is a nonencapsulated, non-demarcated infiltrative neoplasm forming islands, tubules, and acinar structures and loss of polarity with intraluminal papillary projections, supported by a prominent fibrovascular stroma, admixed with areas of necrosis and inflammation characterized by a moderate to high number of viable and degenerate neutrophils, lymphocytes and plasma cells with the

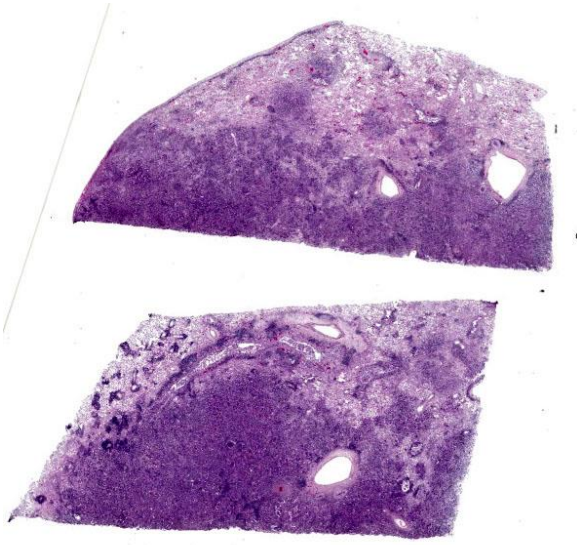

Figure 1-3. Lung, dog. Two sections of lung are submitted for examination. Effacing approximately 66% of the pulmonary architecture is vaguely nodular, unencapsulated, poorly demarcated neoplasm. (HE, 4X)

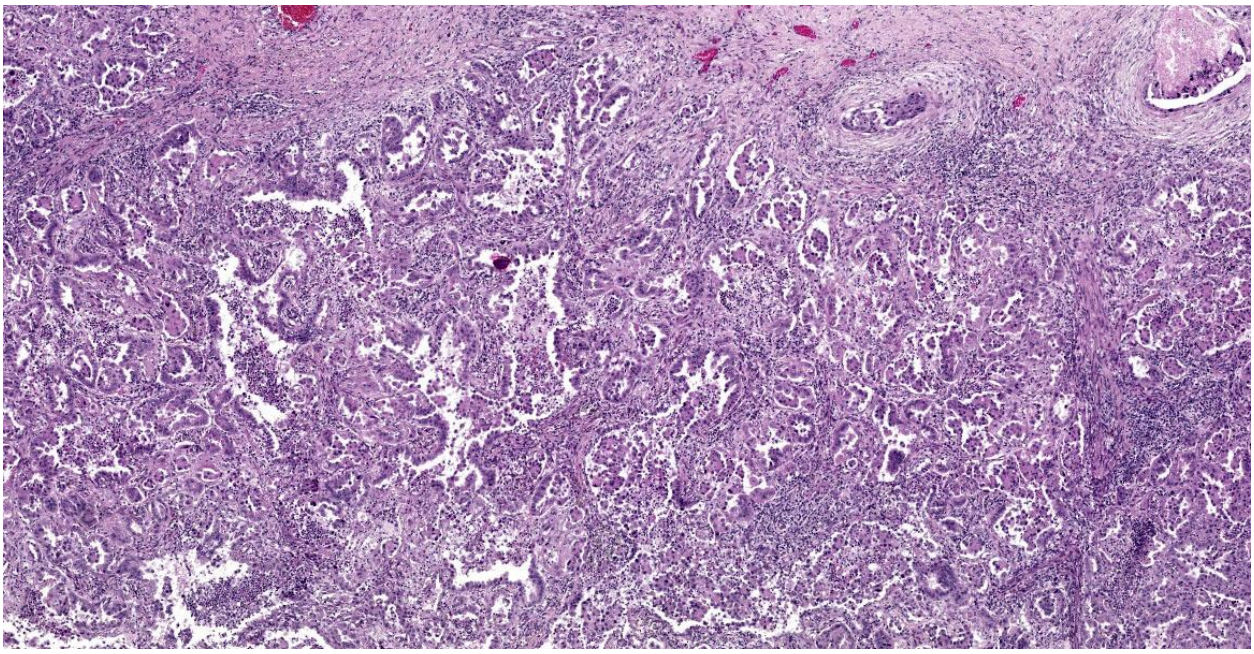

Figure 1-4. Lung, dog. Alveoli, bronchioles, and vessels contain neoplastic cells. (HE, 58X)

odd apoptotic cell. The neoplastic cells are pleomorphic (columnar to polyhedral) and lined the remnant of pulmonary airways with round to oval and basal nuclei. Moderate to high anisocytosis, anisokaryosis, often karyomegaly, and multinucleation with up to three nuclei are noted in the cell population. The cytoplasm of these cells is eosinophilic, finely granular to vacuolated. Mitotic count is 14 per 2.37 mm^2 with atypical mitotic figures. Satellite neoplastic cell clusters are seen in the airways (mostly bronchioles), and lymphovascular invasion is also present. Adjacent to the neoplasm, inside alveolar spaces, there are many foamy macrophages. Diffusely the pleura is expanded by a moderate amount of fibrovascular tissue.

Contributor's Morphologic Diagnosis:
Pulmonary adenocarcinoma, acinar and papillary type.

Contributor's Comment:
Respiratory distress in dogs can be associated with a variety of conditions, including congestive heart failure, upper airway obstruction, and pulmonary tumors. A multimodal approach is often required to investigate the cause of a dyspneic dog. Besides clinical history and physical examination, thoracic radiographs are considered the most important diagnostic test for pets with lung disease because imaging studies can provide a wealth of information on the presence, location, and intensity of the abnormality to guide differential diagnosis and diagnostic plans.[1] Though fine-needle aspiration of the pulmonary parenchyma can be viewed as a relatively invasive technique, it is inexpensive and safe and its result turnaround period is fast and should be considered when evaluating animals with a nodular lung pattern noted on imaging studies.

Primary lung tumors are relatively uncommon in domestic animals. However, pulmonary adenocarcinoma is the most commonly diagnosed primary pulmonary tumor in dogs.[4,6] The most frequent clinical sign associated with pulmonary carcinoma in dogs was coughing (52%), followed by dyspnea (24%), lethargy (18%), and weight loss (12%).[5] How

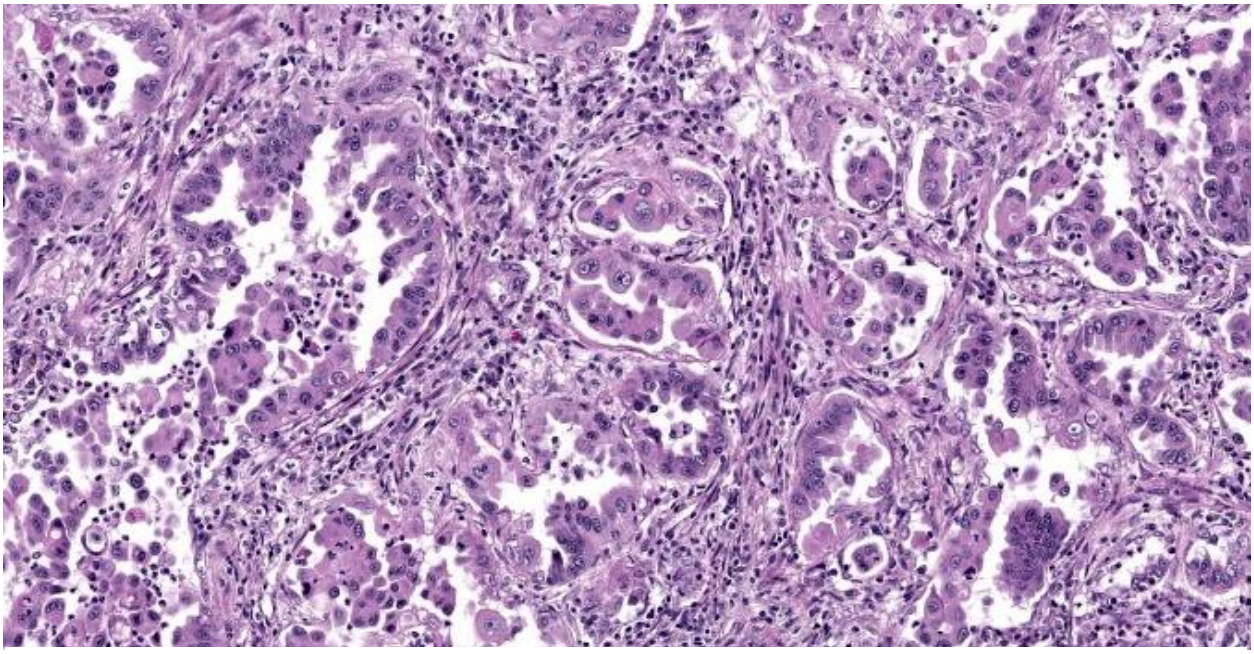

Figure 1-5. Lung, dog. Alveoli and airways are lined by pleomorphic columnar epithelial cells which form papillary projections. There are numerous viable and degenerate neutrophils admixed with cellular debris within some airway lumina that contain neoplastic cells, and numerous lymphocytes and plasma cells within the fibrotic stroma of the neoplasm. (HE, 222X)

ever, in the same survey, 25% of the pulmonary carcinoma cases were incidental findings with no evident clinical signs of respiratory disease before diagnosis.

The lung is also a frequent site for tumor metastasis, and it can sometimes be difficult to differentiate primary pulmonary neoplasms from metastatic neoplasms originating from another location. Immunohistochemistry on thyroid transcription factor-1 (TTF-1) and Napsin A are recommended to confirm the diagnosis of primary pulmonary neoplasia.[7] In the present case, within the lungs, the pulmonary adenocarcinoma had spread through bronchial invasion and re-aspiration with intra-airway seeding in other lobes and lymphovascular invasion The neoplasm also disseminated to the pericardium and esophageal serosa, most likely through direct extension. The fibrous pleuritis was thought to be from the rubbing effects of the neoplasm between the pulmonary and parietal pleura. The hypertrophic osteopathy demonstrated by the thickening of cortical bones is a common paraneoplastic syndrome associated with thoracic space-occupying lesions,[6] of which the exact mechanism is still unknown. The combination of hyperglycemia and mild mature neutrophilia supports that the patient was under stress and, in combination with the mild nonregenerative anemia, likely represented a result of chronic disease, such as cancer.

Contributing Institution:
Department of Biomedical Sciences
Ross University School of Veterinary Medicine, St. Kitts, West Indies
www.veterinary.rossu.edu

JPC Diagnosis:
Lung: Pulmonary adenocarcinoma.

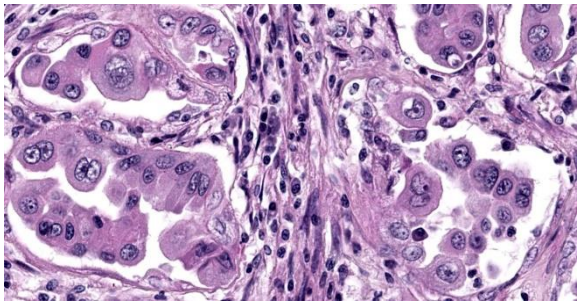

Figure 1-6. Lung, dog. High magnification of pleomorphic neoplastic cells. (HE, 554X)

JPC Comment:
This week's moderator was Dr. Taryn Donovan who is the head of Anatomic Pathology at the Animal Medical Center (AMC) in New York City. The conference cases had a decidedly cardiopulmonary emphasis with the first case being an opportunity to revisit the nomenclature of pulmonary neoplasms. Conference participants noted that the exact pattern of this adenocarcinoma was difficult to pin down with examples of papillary, acinar, and lepidic patterns all within the same neoplasm though this distribution was hardly uniform (figures 1-4 and 1-5). Dr. Donovan emphasized that morphology has diagnostic significance in the human literature[3] though data (and relative importance) is still being weighed in domestic animals. In particular, lepidic patterns (growth along a pre-existing alveolus) may be important if it is the only or predominant pattern as the lack of disruption of the existing pulmonary architecture may include some benign diagnoses such as bronchioalveolar hyperplasia and less aggressive neoplasms (*in situ* and minimally invasive carcinomas) that carry a better prognosis.[3]

Conversely, patterns that disrupt existing pulmonary architecture (e.g. papillary) are far more likely to be associated with an invasive neoplasm and poorer prognosis. Although not conducted for this case, a Verhoeff-Van Gieson stain for elastic fibers may help to illustrate this concept as papillary patterns will lack elastin fibers. Conference participants also discussed micropapillary patterns which are noted to confer the worst prognosis though this nomenclature has not caught on in the veterinary literature. Dr. Donovan described this pattern as 'florettes' with clustering of small numbers of neoplastic cells within alveolar spaces that lacked the more robust stalk of supporting stroma of a true papillary pattern (figure 1-6). Participants also noted evidence of lymphovascular invasion in section with neoplastic cells within a lymphoid vessel, though distinguishing this from an acinar pattern with surrounding myofibroblastic stroma (and an adjacent micropapillary focus) prompted some careful second looks among the group. Dr. Donovan noted 50% of canine and 38% of feline cases in a recent literature meta-review noted a papillary pattern as the predominant morphology of primary pulmonary tumors among the articles[4] reviewed.

As the contributor notes, delineating the origin of pulmonary masses requires consideration of both primary and metastatic neoplasia. We ran IHCs for AE1/3, TTF-1, CK7, Napsin A, vimentin, and P40. Our results mirrored the contributor's (figure 1-7). Neoplastic cells were also modestly immunoreactive for CK7, but not for P40 (marker for squamous differentiation). Altogether, these findings confirm the diagnosis of a primary lung adenocarcinoma. One interesting feature of this case was that select neoplastic cells also expressed vimentin, consistent perhaps with a change in phenotype i.e. epithelial to mesenchymal transition (EMT)[2], though this can also be a feature of poorly differentiated carcinomas as well. EMT of type II pneumocytes is coordinated via cytokines in response to disruption of normal lung architecture – in neoplasia, this also is associated with increased ability of transitioning cells to invade.[2]

Lastly, this case features ancillary diagnostics that are worth a quick look. The contributor

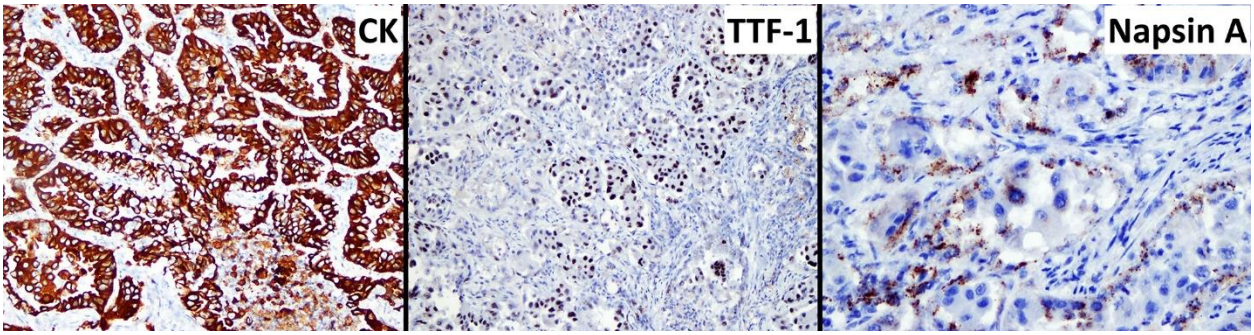

Figure 1-7. Lung, dog. Neoplastic cells demonstrate strong immunopositivity for cytokeratin, and scattered immunopositivity for thyroid transcription factor-1 and napsin A. (*Photo courtesy of:* Ross University School of Veterinary Medicine, St. Kitts, West Indies, www.veterinary.rossu.edu)

provides a solid example of hypertrophic osteopathy (figure 1-1) and representative cytology of a lung aspirate (figure 1-2) that tie this case together.

References:

1. Cohn LA. Diseases of the Pulmonary Parenchyma In: Ettinger SJ, Cote E,Feldman EC, eds. *Textbook of Veterinary Internal Medicine* 8ed: Elsevier Health Sciences 2016.
2. Kobayashi K, Takemura RD, Miyamae J et al. Phenotypic and molecular characterization of novel pulmonary adenocarcinoma cell lines established from a dog. *Nature Sci Rep 13*, 16823 (2023).
3. Kuhn E, Morbini P, Cancellieri A, Damiani S, Cavazza A, Comin CE. Adenocarcinoma classification: patterns and prognosis. *Pathologica*. 2018;110(1):5-11.
4. McPhetridge JB, Scharf VF, Regier PJ, et al. Distribution of histopathologic types of primary pulmonary neoplasia in dogs and outcome of affected dogs: 340 cases (2010-2019). *J Am Vet Med Assoc* 2021;260:234-243.
5. Ogilvie GK, Haschek WM, Withrow SJ, et al. Classification of primary lung tumors in dogs: 210 cases (1975-1985). *Journal of the American Veterinary Medical Association* 1989;195:106-108.
6. Wilson DW. Tumors of the respiratory tract In: Meuten DJ, ed. *Tumors in domestic animals*. Ames Iowa, USA: Wiley Blackwell, 2017;467-498.
7. Ye J, Findeis-Hosey JJ, Yang Q, et al. Combination of napsin A and TTF-1 immunohistochemistry helps in differentiating primary lung adenocarcinoma from metastatic carcinoma in the lung. *Appl Immunohistochem Mol Morphol* 2011;19:313-317.

CASE II:

Signalment:
4-month-old, intact male mixed breed dog (*Canis lupus familiaris*).

History:
This animal had severe upper respiratory signs with green nasal discharge, severe conjunctivitis, lethargy, loss of appetite and dehydration.

Gross Pathology:
Examined is a 5.75 kg, juvenile (4-months-old) intact male mixed breed dog in good postmortem condition. A moderate amount of thin red-tinged transparent fluid exudes from the nasal and oral cavities. There is some mild frond-like proliferation of the skin on the dorsal nasal planum. The nasal turbinates are mostly reddened. There is negative pressure and approximately 125 mL of semi-

Figure 2-1. Lung, dog. The lungs fail to collapse, are diffusely dark red to purple, firm and contain innumerable pinpoint white nodules. (*Photo courtesy of:* University of Illinois at Urbana-Champaign, Veterinary Diagnostic Laboratory, http://vetmed.illinois.edu/vet-resources/veterinary-diagnostic-laboratory/)

translucent to slightly cloudy, thin, red-tinged fluid within the pleural cavity. The lungs fail to collapse, are diffusely dark red to purple, firm and contain innumerable pinpoint, firm, white nodules scattered throughout all lung lobes. A few sections float in formalin while a few sections sink. The tracheobronchial lymph nodes are subjectively enlarged and are diffusely dark red. The stomach contains a small amount of watery, tan fluid and the rugal folds are prominent. The intestinal tract contains a scant amount of tan watery ingesta. The colon is empty. The serosal surfaces of the intestinal tract have a subtle ground glass appearance.

Laboratory Results:

1. Aerobic culture (lungs): Escherichia coli (moderate growth), Staphylococcus pseudintermedius (moderate growth)
2. Canine Adenovirus (CAdV) 1 and 2 PCR (lung): Negative
3. Canine Distemper Virus (CDV) PCR (lung): Positive
4. Canine Herpesvirus 1 PCR (lung): Negative
5. Influenza A PCR (lung): Negative

Microscopic Description:

Lung: Multifocally and randomly scattered throughout the parenchyma are numerous loosely nodular aggregates of amorphous to granular eosinophilic debris (necrosis) that replaces the normal architecture. Areas of necrosis are characterized by accumulations of small basophilic granules (karyorrhectic debris), eosinophilic ghosts of necrotic round cells, extravasated erythrocytes (hemorrhage), abundant hypereosinophilic granular to fibrillar material (fibrin), and low numbers of degenerate macrophages. The adjacent alveolar spaces are often filled by plump and foamy macrophages, low numbers of neutrophils, and occasional sloughed degenerate epithelial cells mixed with hemorrhage, eosinophilic wispy material (edema) and fibrin. Scattered throughout examined sections and distending the cytoplasm of macrophages, alveolar epithelial cells or occasionally free within the tissues adjacent to disrupted macrophages are occasional to few, variably sized dense clusters of protozoal organisms. Organisms are round to fusiform, 2-4 µm in diameter and contain a small, central basophilic nuclear body. Rarely, viable and sloughed alveolar and bronchiolar epithelial

Figure 2-2. Lung, dog. A single section of lung is submitted for examination. Airways and alveoli are diffusely filled with a cellular exudate. (HE, 4X)

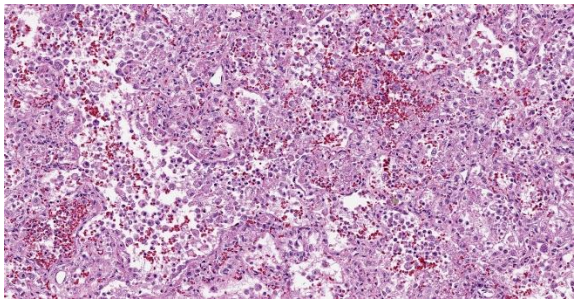

Figure 2-3. Lung, dog. The exudate filling all air spaces is primarily macrophages with fewer neutrophils, abundant polymerized fibrin, and cellular debris. (HE, 187X)

cells contain small, eosinophilic intranuclear or intracytoplasmic viral inclusion bodies. Few bronchioles contain variable numbers of degenerate neutrophils and macrophages mixed with necrotic debris. The respiratory epithelium lining these bronchioles is often hypocellular and remaining epithelial cells are flattened (attenuated) or angular with moth-eaten cytoplasm and pyknotic nuclei (necrosis).

Immunohistochemical (IHC) staining of organisms in the lungs with an antibody targeting *Toxoplasma spp.* is performed. Numerous intracytoplasmic discrete clusters and scattered individual 2-4 µm diameter protozoal organisms exhibit positive immunostaining.

Other histopathology findings that are not included in the provided slide include:

- Hyperkeratosis of the nasal planum
- Lymphoplasmacytic conjunctivitis with rare viral inclusion bodies
- Toxoplasma organisms in the bone marrow, thyroid gland, and spleen
- Splenic lymphocytolysis
- Viral inclusions in mononuclear cells of mesenteric lymph node

Contributor's Morphologic Diagnosis:
Lungs: Severe, multifocal to coalescing, necrotizing bronchointerstitial pneumonia with intranuclear and intracytoplasmic viral inclusion bodies and intracytoplasmic protozoal organisms consistent with *Toxoplasma spp.*

Contributor's Comment:
Canine distemper virus (CDV) is caused by a Morbillivirus (family Paramyxoviridae)[2] and has been shown to infect a wide variety of carnivores, including members of Canidae (domestic and wild dogs), Mustelidae (ferrets, mink), wild members of Felidae, raccoons[6] and skunks.[1] In addition to many terrestrial carnivores, some species of seals are also susceptible,[2] including Caspian seals.[8] In dogs, virus is transmitted through infected bodily tissues,[12] particularly respiratory secretions.[2] Within the upper respiratory tract, virus is phagocytosed by mucosal lymphocytes and macrophages, which travel to the tonsils and local lymph nodes. Here, the virus continues to replicate, infecting more lymphocytes and macrophages which then spread systemically.[12] Within 2-5 days of exposure, the virus has spread throughout the body and can be found in various lymphoid tissues including bone marrow, thymus, and intestinal lymphoid tissues.[2] Once within lymphoid tissues, the virus can then spread to and infect epithelial and mesenchymal (pantropic) cells throughout the body, particularly within the respiratory, nervous and alimentary systems.[12]

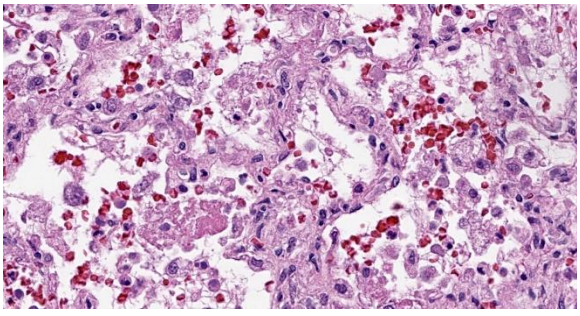

Figure 2-4. Lung, dog. High magnification of alveolar septa and lumina demonstrating the luminal exudate and the expansion of alveolar septa by inflammatory cells, edema, and hyperplastic type II pneumocytes. (HE, 554X)

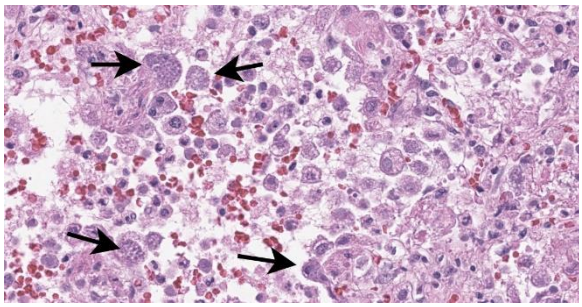

Figure 2-5. Lung, dog. Numerous cell types, including airway epithelium, alveolar macrophages, and Type II pneumocytes contain a large cytoplasmic cyst with numerous 2-3um round zoites consistent with *Toxoplasma gondii* (arrows). (HE, 554X)

Within the respiratory tract, viral infection leads to death of pneumocytes, bronchiolar epithelium and macrophages, leading to impaired oxygen exchange, removal of debris and potential infectious organisms and decreased phagocytic and antigen-presenting ability by macrophages.[12] Grossly, lesions of the respiratory tract include mucopurulent exudate within the nasopharynx as well as bronchointerstitial pneumonia characterized by patchy to diffuse red-tan, rubbery lesions,[2] both of which are seen in this case. Histologically, mild suppurative inflammation within bronchioles as well as necrosis, attenuation of bronchiolar epithelium and intracytoplasmic (rarely, intranuclear outside of the nervous system) inclusion bodies may be observed.[2]

An important potential consequence of CDV infection is immune suppression and increased susceptibility to co-infections.[2] Infection of and consequential cell death of lymphocytes and macrophages leads to lymphoid depletion of the thymus, lymph nodes, tonsils and various mucosal-associated lymphoid tissues. Various secondary infections have been documented in dogs including bacterial (*Bordetella*, *Rhodococcus equi*), viral (adenovirus), fungal (*Pneumocystis*, *Cryptosporidium*), and protozoal (*Toxoplasma*, *Sarcocystis*, *Neospora*).[2,4,9,10] Immune suppression and secondary infections also play an important role in CDV infections in many other species with co-infections of *Sarcocystis* and *Toxoplasma* reported in raccoons and skunks,[1,5,7] and *Toxoplasma* in mink, ferrets, and gray foxes.[7]

Toxoplasma gondii is an obligate intracellular coccidian protozoal organism[9] that utilizes felid species as its definitive hosts but can likely cause disease in any mammal.[11] Sexual reproduction only occurs within the feline gastrointestinal tract and infectious oocysts are released into the environment in feces. Transmission to other species occurs through ingestion of infected feces within the environment.[11] In most immunocompetent hosts, *Toxoplasma* does not cause clinical disease, but with immune suppression particularly in young hosts, can lead to systemic toxoplasmosis. Dissemination of infectious tachyzoites occurs in various immune cells (lymphocytes, macrophages, granulocytes) or freely within the blood.[11] Within the lungs, *Toxoplasma* infection is typically characterized grossly by small, white foci scattered throughout the parenchyma.[2] Histologically, multifocal necrotizing interstitial pneumonia with histiocytic and neutrophilic infiltrates and Type II pneumocyte hyperplasia may be observed.[6]

Contributing Institution:
University of Illinois at Urbana-Champaign, Veterinary Diagnostic Laboratory
http://vetmed.illinois.edu/vet-resources/veterinary-diagnostic-laboratory/

JPC Diagnosis:
Lungs: Pneumonia, bronchointerstitial, fibrinonecrotizing and histiocytic, chronic, diffuse, severe with intranuclear and intracytoplasmic viral inclusions, and intracellular and extracellular protozoa.

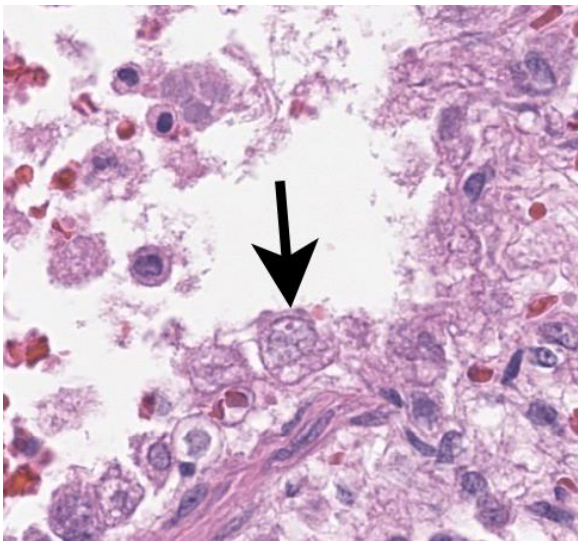

Figure 2-6. Lung, dog. Rarely, remnant airway epithelial cells (arrow) and alveolar macrophages contain one or more small 2-4um irregularly round eosinophilic cytoplasmic inclusions. (HE, 713X)

JPC Comment:
This second case is a wonderful example of an interstitial pneumonia that is generous enough to have two separate entities present at the same time (figures 2-3 and 2-4)! We performed modified Gram stains (Brown-Brenn, Brown-Hopps) that confirmed the bacterial culture results for this case, particularly within the larger airways that contained necrotic debris and neutrophilic inflammation. Though this was a minor feature for this case, it fits with the overall immunosuppression related to canine morbillivirus that the contributor nicely outlines. Both Giemsa and PAS stains highlighted intrahistiocytic and intraalveolar cysts of *Toxoplasma*, though these were also readily apparent on H&E alone (figure 2-5). The presence of viral particles within select alveolar and bronchiolar epithelial cells was subtle (figure 2-6), though conference participants noted convincing intranuclear and intracytoplasmic inclusions. Conference participants also discussed whether there were viral syncytial cells present but were not confident that these could be distinguished from multinucleated giant cell macrophages. One takeaway from this case is that necrotizing pneumonias where *Toxoplasma* is suspected should prompt a careful search for an inciting cause for immunosuppression with canine morbillivirus having recognizable features in section. There are several major risk factors for canine toxoplasmosis. As the contributor notes, primary disease is associated with immunosuppression.[3] Seroprevalence estimates from around the world vary, though national estimates vary from 7.9% to 42.8% of dogs.[3] Cohabitation of dogs with cats (the definitive host) is associated with greater seroprevalence as is outdoor housing of dogs and coprophagy habits. With these data in mind, exposure of dogs to *Toxoplasma* is a likely event in many environments though immunocompetent animals are typically subclinically infected and do not exhibit signs. The role of vaccination and the possibility of diminished maternal immunoglobulins from poor transfer or lack thereof is worth noting for this case, though the history for this animal is sparse.

References:
1. Burcham GN, Ramos-Vara JA, Vemulapalli R. Systemic Sarcocystosis in a Striped Skunk (Mephitis mephitis). *Veterinary Pathology*. 2010;47(3):560-564.
2. Caswell JL, Williams KJ. Respiratory System. ln: Maxie MG ed. *Jubb, Kennedy, and Palmer's Pathology of Domestic Animals*. Vol. 2. 6th ed. Philadelphia, PA: Elsevier Saunders. 2016: 574-576, 590.
3. Dini FM, Stancampiano L, Poglayen G. et al. Risk factors for Toxoplasma gondii infection in dogs: a serological survey. *Acta Vet Scand*. 2024;66(14).
4. Headley, SA, Oliveira TES, Pereira AHT, Moreira JR, et al. Canine morbillivirus (canine distemper virus) with concomitant canine adenovirus, canine parvovirus-2, and Neospora caninum in puppies: a retrospective

immunohistochemical study. *Nature Scientific Reports.*
5. Kubiski SV, Sisó S, Church ME, Cartoceti AN, Barr B, Pesavento PA. Unusual Necrotizing Encephalitis in Raccoons and Skunks Concurrently Infected with Canine Distemper Virus and Sarcocystis sp. *Veterinary Pathology*. 2016;53(3):674-676.
6. Lopez A. Respiratory System, Mediastinum and Pleurae. Ln: McGavin MD, Zachary JF eds. *Pathologic Basis of Veterinary Disease*. 5th ed. St. Louis, MO: Mosby Elsevier; 2012: 524-527.
7. Moller T, Nielsen SW. Toxoplasmosis in Distemper-Susceptible Carnivora. *Pathologia veterinaria*. 1964; 1(3): 189-203.
8. Namroodi S, Shirazi AS, Khaleghi SR, N. Mills J, Kheirabady V. Frequency of exposure of endangered Caspian seals to Canine distemper virus, Leptospira interrogans, and Toxoplasma gondii. PLoSONE. 2018;13(4).
9. Portilho FVR, Paes AC, Megid J, Hataka A, et al. Rhodococcus equip VAPN type causing pneumonia in a dog coinfected with canine morbillivirus (distemper virus) and *Toxoplasma gondii*. *Microbial Pathogenesis*. 2019; 129: 112-117.
10. Postma GC, Dellarupe A, Streitenberger N, Bratanich A, et al. Canine distemper virus, atypical Toxoplasma gondii, and Neospora caninum co-infection, in a dog with neurological signs from Argentina. *Brazilian Journal of Veterinary Pathology*. 2019; 12(3): 101-105.
11. Uzal FA, Plattner BL, Hostetter JM. Alimentary System. ln: Maxie MG ed. *Jubb, Kennedy, and Palmer's Pathology of Domestic Animals*. Vol. 2. 6th ed. Philadelphia, PA: Elsevier Saunders. 2016: 236-237.
12. Zachary JF. Mechanisms of Microbial Infections. Ln: McGavin MD, Zachary JF eds. *Pathologic Basis of Veterinary Disease*. 5th ed. St. Louis, MO: Mosby Elsevier; 2012: 226-227.

Figure 3-1. Heart, dog. Coronary blood vessels visible on the epicardium are thickened and yellow. (*Photo courtesy of:* Department of Biomedical Sciences and Pathobiology, Virginia Maryland College of Veterinary Medicine, https://vetmed.vt.edu/departments/biomedical-sciences-and-pathobiology.html)

CASE III:

Signalment:
A 13-year-old, neutered male, German Shepherd dog (*canis familiaris*)

History:
The patient had a history of hip dysplasia clinically diagnosed when the animal was 7-years-old and a fully excised mast cell tumor when this dog was 10-years-old. This animal always had good body condition. Animal was found dead without premonitory signs.

Gross Pathology:
The body had good post mortem preservation and good nutritional status, with ample deposits of adipose tissue in the subcutis and body cavities. There were large amounts of fibrin and alimentary contents in the abdominal cavity. In the gastric wall, a focal perforated transmural ulcer was identified in the fundic area. The lungs were red and wet. The myocardium was slightly pale and the

Figure 3-2. Heart, dog. Sections from the right (top) and left ventricles are submitted for examination. In both sections, the walls of coronary arteries and smaller arterioles are markedly thickened. (HE, 5X)

coronary blood vessels visible on the epicardium were thickened with a yellow, irregular plaque-like lesions. No significant findings in other internal organs.

Microscopic Description:
Heart, right and left ventricle: The most significant findings were identified in large and medium size arteries located in all layers of the heart. They all exhibit severe atheromatosis, characterized by the presence of numerous cholesterol clefts and foamy macrophages within the sub intima and/or in the adventitia of the vessels. In these areas, there are variable amounts of fibrin within the sub intima (fibrinoid necrosis) and also attached to the endothelial surface (thrombosis), and extensive hemorrhages and numerous hemosiderin laden macrophages. Some vessels are completely occluded with this inflammatory reaction. In the myocardium, multifocal areas of interstitial fibrosis are noted. In the sample collected from the right ventricle, there are numerous adipocytes tracking along the vessels in the myocardium (likely as a reflection of body condition).

Contributor's Morphologic Diagnosis:
Heart: Atherosclerosis, severe, multifocal, with foamy macrophages, cholesterol clefts and multifocal mild myocardial fibrosis.

Contributor's Comment:
Multiple vessels in different organs (including the stomach, kidney, brain, lung, liver and small intestine) displayed atherosclerosis. This vascular lesion probably predisposed to an area of gastric ischemia/hypoxia, with consequent necrosis and rupture of the stomach. The cause for atherosclerosis in this patient could not be elucidated, due to the absence of antemortem blood studies. No significant gross or histologic findings were identified in the thyroid gland, adrenal gland, or pancreas.

Atherosclerosis is defined as a focal or multifocal thickening of the arterial walls due to the deposition of lipids, forming plaques.[6,7] This condition has been associated with hyperlipidemia, which is defined as an elevation of plasma concentration of triglycerides and/or cholesterol. Hyperlipidemia can be physiologic or pathologic. Physiologic hyperlipidemia is frequently observed after meals (post prandial). Pathologic hyperlipidemia is associated with cholestasis, high fat diets, drug administration, nephrotic syndrome,

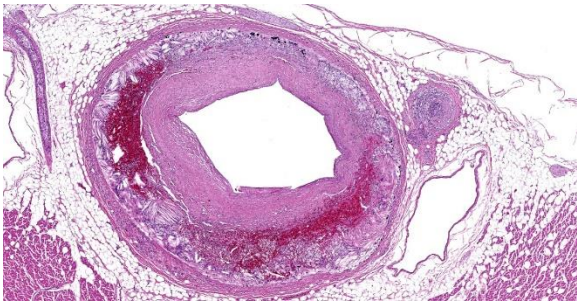

Figure 3-3. Heart, dog. There is marked intimal hyperplasia and the tunica media is markedly expanded by acicular cholesterol clefts admixed with large numbers of foamy macrophages, hemorrhage, and mineral. (HE, 34X)

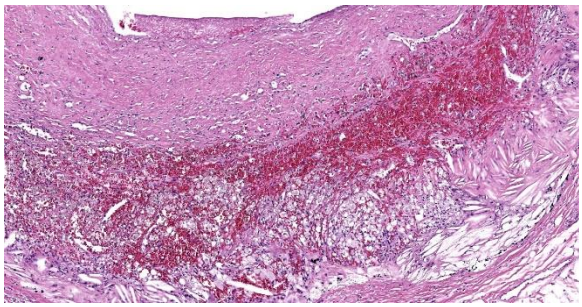

Figure 3-4. Heart, dog. Higher magnification of the arterial wall. (HE, 103X)

lymphoma or endocrinopathies, such as hypothyroidism, hyperadrenocorticism and diabetes mellitus.[5,9,11]

In domestic species, rabbits, chickens and pigs ae considered "atherosensitive", whereas dogs, cats, ruminants and rats are considered "atheroresistant".[9] In dogs, atherosclerosis is almost always present in association with hypothyroidism or diabetes mellitus, although canine hypertension and obesity has also been associated with this condition. Spontaneous atherosclerosis has also been described but is considered extremely rare.[5]

The pathogenesis of atherosclerosis is not completely nor well understood.[2] Dogs with hypothyroidism have increased very low-density lipoproteins (VLDL), low density lipoproteins (LDL) and high-density lipoproteins (HDL). Dogs with diabetes mellitus have increased VLDL and HDL, and dogs with hyperadrenocorticism have increased LDL.[1] As a result of hyperlipidemia, endothelial injury/dysfunction may occur.[9] Endothelial cell dysfunction is defined as non-adaptive alteration in functional phenotype, which are fundamental in the regulation of hemostasis and thrombosis, local vascular tone, redox balance and inflammatory reaction. This dysfunction allows focal permeating, trapping and physicochemical modifications of circulating lipoprotein particles in the subendothelial space.[10] This sequence of events leads to platelet adhesion, monocyte adhesion and infiltration, and insudation of lipid, as extracellular lipid or as intracellular lipid in "foam cells". In addition, multiple growth factors and chemokines are generated by activated macrophages and endothelial cells, which activate smooth muscle cells and their precursors to promote their proliferation and synthesis of extracellular matrix in the intimal compartment. In one individual, numerous atherosclerotic plaques can coexist, and each has their own pathobiological evolution.[4,9]

The histopathologic lesion of atherosclerosis in dogs differs from the human counterpart, as the lesion in dogs has been described to begin in the middle and outer layers of the media and is much more frequent in small muscular arteries. The deposition of lipids in the internal layers of the media can promote disruption of the internal elastic lamina and involvement of the intima. In humans, atherosclerosis is primarily present in the intima and may extend to the tunica media and adventitia.[9] Veins are not affected. Reports of immunohistochemical analysis of the atheromatous plaques in dogs conclude that lipids in the lesions contained low density lipoproteins, so they have similar features to human atherosclerotic lesions.[6]

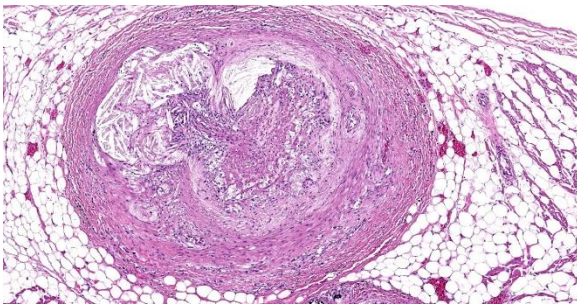

Figure 3-5. Heart, dog. In some vessels, the lumen is seriously compromised by aggregates of cholesterol clefts and macrophages. (HE, 103X)

Grossly, the lesions are identified as multifocal, sometimes confluent, yellow brown nodules in arterial walls in different organs. The heart, kidney and brain are usually more severely involved.[9] Miniature Schnauzers (particularly females) and Shetland sheepdogs are predisposed to primary hyperlipidemia and are considered to be breeds with high risk for developing atherosclerosis.[8]

Atherosclerosis can be confirmed by histopathology. Nevertheless, because of invasiveness of sampling, the use of diagnostic imaging (CT scanner) may be used to assess the antemortem presence of calcified atheromatous plaques and degree of damage. This technique is useful in animals without evidence of metastatic calcification or endocrinopathy.[7]

Contributing Institution:
Department of Biomedical Sciences and Pathobiology
Virginia Maryland College of Veterinary Medicine
205 Duck Pond Drive
Blacksburg, VA 24061.
https://vetmed.vt.edu/departments/biomedical-sciences-and-pathobiology.html

JPC Diagnosis:
Heart: Atherosclerosis, chronic, diffuse, severe with multifocal cardiomyocyte loss and fibrosis.

JPC Comment:
The contributor provides a detailed look at atherosclerosis that accompanies a great gross photo (figure 3-1) and a nice histology slide as well. The changes within muscular arteries are superb and are conveniently laid out both in cross-section and longitudinal section with a constellation of changes to appreciate (figures 3-2, 3-3, 3-4). Conference participants were also interested in the infil

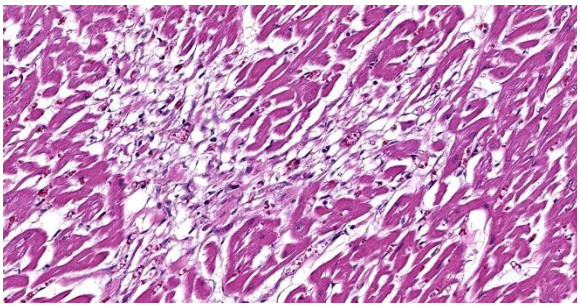

Figure 3-6. Heart, dog. There are scattered areas of myofiber loss, atrophy, and replacement fibrosis.

tration of adipocytes within the right ventricle and discussed the ultimate genesis. While arrhythmogenic right ventricular cardiomyopathy (ARVC) is a good differential for this case due to the concurrent fibrous and fatty appearance of this section, myocytes lack active degeneration/necrosis that would be expected with ARVC. Instead, another potential explanation for these changes is ischemic injury to myocytes with loss and fibrosis – the infiltration of adipocytes in a generously apportioned *(syn*: extremely well-fed) reflects a race to see which entity will fill the empty space up first.

We ran Movat's and Masson's chromatic stains to characterize vascular and perivascular changes in this case. There is narrowing to complete occlusion of the vascular lumina (figure 3-5) with marked disruption of the tunica intima to include a focal area with fibrin and hemorrhage that may represent a true rupture of the coronary artery. Recently, a similar case of atherosclerosis was reported in a dog that lacked a history of endocrinopathy with distribution of lesions centered solely on the abdominal aorta and renal vasculature.[3] The only clinical signs attributable in that presentation however were a history of hindlimb paresis and elevated renal values; primary cardiac lesions were absent grossly and histologically. Lastly, the distribution of lesions in this case (primarily subintimal) should be contrasted with atherosclerosis in

birds where the lesions occur primarily within the intima as stiff plaques. For an example of recent WSC, refer to Conference 6, Case 1, 2023-2024 for a contrasting case in a saker falcon.

References:

1. Barrie J, Watson TDG, Stear MJ et al. Plasma cholesterol and lipoprotein concentrations in the dog: The effects of age, breed, gender, and endocrine disease. *J Sm Anim Pract*. 1993; 34: 507-512.
2. Boynosky NA, Stokking L. Atherosclerosis associated with vasculopathic lesions in a golden retriever with hypercholesterolemia. *Can Vet J*. 2014; 55: 484-488.
3. Gimbrone MA Jr, García-Cardeña G. Endothelial Cell Dysfunction and the Pathobiology of Atherosclerosis. *Circ Res*. 2016; 118: 620-636.
4. González-Domínguez, A, Tormo JR, Herrería-Bustillo, VJ. Aortic thrombosis and acute kidney injury due to atherosclerosis in a dog. *JAVMA*. 2024; 262(8):1-4.
5. Hess RS, Kass PH, Van Winkle TJ. Association between diabetes mellitus, hypothyroidism or hyperadrenocorticism, and atherosclerosis in dogs. *J Vet Intern Med*. 2003; 17: 489-494.
6. Kagawa Y, Hirayama K, Uchida E et al. Systemic atherosclerosis in dogs: histopathological and immunohistochemical studies of atherosclerotic lesions. *J Comp Pathol*. 1998; 118: 195-206.
7. Lee E, Kim HW, Bae H, et al. Radiography and CT features of atherosclerosis in two miniature Schnauzer dogs. *J Vet Sci*. 2020; 21: e89.
8. Mori N, Lee P, Muranaka S, et al. Predisposition for primary hyperlipidemia in miniature Schnauzers and Shetland sheepdogs as compared to other canine breeds. *Res Vet Sci*. 2010; 88: 394-399.
9. Robinson WF, Robinson NA. Cardiovascular System. In: Maxie MG, ed. Jubb, Kennedy & Palmer's Pathology of Domestic Animals. Vol 3. 6th ed. St. Louis, MO: Elsevier; 2016:1-101.
10. Simionescu N, Vasile E, Lupu F, et al. Prelesional events in atherogenesis. Accumulation of extracellular cholesterol-rich liposomes in the arterial intima and cardiac valves of the hyperlipidemic rabbit. *Am J Pathol*. 1986; 123: 109-25.
11. Watson TDG, Barrie J. Lipoprotein metabolism and hyperlipidaemia in the dog and cat: A review. *J Sm Anim Pract*. 1993; 34: 479-487.

CASE IV:

Signalment:
1-year-old, spayed female, domestic shorthair cat (*Felis catus*)

History:
This patient presented to the Cardiology Service for evaluation of a heart murmur. An angiogram diagnosed a large, bidirectional patent ductus arteriosus (PDA). On subsequent recheck echocardiograms, shunting transitioned between left-to-right and bidirectional, as well as showed progressive right ventricular hypertrophy. Abdominal ultrasound showed development of mild ascites. At final presentation, this patient developed marked abdominal effusion and abdominocenteses with fluid analysis revealed a high-protein, exudative effusion. Euthanasia was elected due to progressive vomiting and anorexia.

Gross Pathology:
Examination of the lungs is after formalin fixation. The visceral pleura is multifocally expanded by dozens of sharply demarcated, pinpoint to 0.4 cm in diameter, hemispheric, white-tan nodules. On section, the lungs contain dozens of poorly demarcated, firm, tan areas. Lung lobes sections float in formalin.

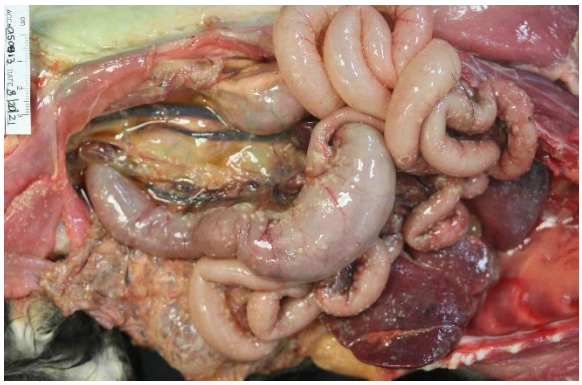

Figure 4-1. Abdominal viscera, cat. There are numerous tan-yellow nodules over the abdominal surfaces which range from pinpoint to 1 cm x 0.6 cm x 0.6 cm. (*Photo courtesy of:* Schwarzman Animal Medical Center, http://www.amcny.org/)

Extrapulmonary lesions include myriads of multifocal to coalescing, hemispheric, tan-yellow nodules over the peritoneum, omentum, serosa, splenic capsule, hepatic surface, renal capsules, and renal cortices, which range from pinpoint to 1 cm x 0.6 cm x 0.6 cm. Nodules often track along mesenteric and renal subcapsular veins. The mesenteric, hepatic, pancreaticoduodenal, and colonic lymph nodes are moderately to severely enlarged and the cut surfaces contain dozens of coalescing, poorly demarcated, tan-yellow regions. Within the abdominal cavity is approximately 80 mL of a viscous, mildly turbid, yellow fluid mixed with dozens of gelatinous, semi-translucent, yellow strands that are loosely adhered to the viscera (fibrin). The serosae are rough and dull and hepatic and splenic capsules are multifocally cloudy and dull.

Laboratory Results:
Albumin: 1.9 g/dL (reference 2.6 - 3.9 g/dL)
Globulin: 6.2 g/dL (reference 3.0 - 5.9 g/dL)
Albumin: Globulin Ratio: 0.3
Abdominal effusion: Fluid analysis: high-protein (greater than 4.0 g/dL), exudative effusion
Abdominal Fluid - Feline Coronavirus Real-PCR: Positive (Biotype FECV)

Microscopic Description:
Lungs: The submitted sections of lung show multiple overlapping pathologic processes. The pleura is multifocally elevated and expanded by an acellular, fibrillar, eosinophilic material (fibrin) mixed with karyorrhectic debris (necrosis) and moderate to large numbers of lymphocytes, plasma cells, macrophages, and neutrophils. Inflammation infiltrates and expands the subjacent alveolar septa, which are frequently lined by hyperplastic type II pneumocytes. Expanding and infiltrating the remaining alveolar septa are moderate numbers of macrophages, lymphocytes, plasma cells, and neutrophils with rare type II pneumocyte hyperplasia. Filling the alveolar spaces is variable pale eosinophilic (seroproteinaceous) fluid, extracellular bacteria (mixed morphologies), increased intra-alveolar macrophages, and intra-alveolar protein. Small to medium-sized pulmonary arteries/arterioles display multiple pathologic changes. The tunica intima and subintima are partially to circumferentially expanded by a homogenous, eosinophilic matrix (fibrosis). The tunica media is multifocally expanded by fibrosis and/or increased numbers of hypertrophied smooth muscles cells (muscular hypertrophy) that cause compression/obliteration of the vascular lumens. Vascular lumens are commonly bridged and filled by plexiform lesions characterized by sieve-like masses comprised of a core of an extracellular matrix, smooth muscle cells, and stromal cells lined by quiescent and hypertrophied endothelial cells. When longitudinally sectioned, plexiform lesions are prominent at branch points. Variable expansion of the tunica adventitia is by either concentric dense or loose onion-skin fibrosis. Multiple blood vessels are moderately to severely distended by sac-like dilations (highlighted by Masson's Trichrome stain). Intermittent blood vessels are cuffed by mild to moderate numbers of lymphocytes, plasma cells, macro-

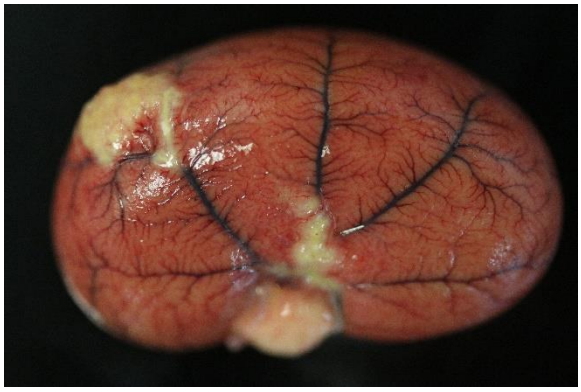

Figure 4-2. Kidney, cat: Nodules track along the renal subcapsular vein. (*Photo courtesy of:* Schwarzman Animal Medical Center, http://www.amcny.org/)

phages, and neutrophils. Separating the perivascular adventitia and tissues are clear spaces and an acellular, pale eosinophilic fluid (edema). There is multifocal, mild to moderate vascular congestion. Occasional macrophages contain morphologically separate intrahistiocytic pigments and foreign material (carbon, silica, hemosiderin, and/or lipofuscin).

Immunohistochemical stain for **FIPV** (Animal Health Diagnostic Center/Cornell University) revealed strong cytoplasmic immunoreactivity of macrophages within pleural granulomas.

Contributor's Morphologic Diagnosis:
Lungs:

1) Pulmonary arteriopathy, chronic, multifocal, severe with multifocal, mild to moderate, intimal, subintimal, medial, and adventitial fibrosis; moderate to marked medial hypertrophy; multifocal plexiform lesions; and multifocal, moderate to marked vascular dilation
2) Pleuritis and interstitial pneumonia, fibrinonecrotizing, histiocytic, lymphoplasmacytic, neutrophilic, chronic, multifocal to coalescing, moderate with regional type II pneumocyte hyperplasia
3) Interstitial pneumonia, histiocytic, lymphoplasmacytic, neutrophilic, chronic, diffuse, moderate with multifocal type II pneumocyte hyperplasia, alveolar histiocytosis, and minimal intra-alveolar protein
4) Edema, diffuse, mild to moderate

Contributor's Comment:
Microscopic examination in this case revealed two distinct pathologic processes consistent with concurrent feline infectious peritonitis virus (FIPV) infection and plexogenic pulmonary arteriopathy. Additional findings consistent with FIPV infection included high-protein abdominal effusion, multiorgan and body cavity inflammatory nodules, fibrinonecrotizing phlebitis, and pleocellular lymphadenitis. Immunohistochemistry confirmed FIPV within lesions. In this patient, systemic-to-pulmonary shunting through the PDA resulted in the prominent plexiform arteriopathy.

Coronaviruses infect a wide-range of wild and domestic species, where they are associated with respiratory, reproductive, gastrointestinal, and systemic diseases.[1,7,8,11-14,17] Virions are enveloped and contain large (80-220 nm), positive-sense, single-stranded RNA genome.[7,8,11,14,17] Viral proteins include 3-4 structural proteins (spike glycoprotein (S), transmembrane glycoproteins (M and E), nucleoprotein (N), and inconstant hemagglutinin (HE)) and non-structural accessory proteins.[7,8,11,17] Club-shaped spike glycoproteins (S) form a characteristic radiating crown-appearance on ultrastructure. [7,8,11] These spike proteins mediate receptor binding and fusion at the plasma membrane or endosomes facilitating viral entry.[7,8,11,14] Thus, the host range and cell tropism is predominantly determined by the spike (S) protein.[7,8,11,14] In addition, spike proteins participate in induction antibody and cell-mediated responses.[8] Coronaviruses exhibit a high mutation rate due to

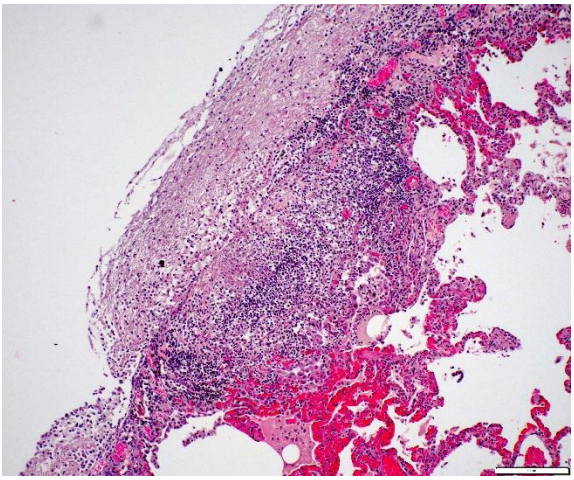

Figure 4-3. Lung, cat. Inflammation infiltrates and expands the subjacent alveolar septa, which are frequently lined by hyperplastic type II pneumocytes. (HE, 200X) (*Photo courtesy of:* Schwarzman Animal Medical Center, http://www.amcny.org/)

RNA-polymerase transcription errors and genetic recombination between related coronavirus during coinfections.[8,11,13,14] Feline coronaviruses (FCoVs) belongs to the family Coronaviridae within the alphacoronavirus genus.[7,8,11,17] Other important alphacoronaviruses in veterinary medicine include canine coronavirus, TGE virus of swine, porcine epidemic diarrhea virus (PEDV), porcine respiratory coronavirus, alpaca respiratory coronavirus, and ferret and mink coronaviruses.[7,11] There are two main circulating serotypes of feline coronaviruses (FCoVs): the predominant serotype I and rare serotype II.[7,8,11,13,14,17] Infection with serotype II is initiated through binding of the host aminopeptidase N receptor but the receptor for serotype I remains unknown.[7,8,11,13,17] A potential other host receptor, dendritic cell-specific ICAM (DC-ICAM), has been suggested for both serotypes.[7,8,13]

Feline coronaviruses (FCoV) include two separate biotypes: feline enteric coronavirus (FECV) and feline infectious peritonitis virus (FIPV).[1,7,8,11,12] FECV infects and replicates in the intestinal epithelium and is generally associated with a self-limiting, mild gastroenteritis.[1,8,11-13] A severe catarrhal and hemorrhagic enteritis can be seen in juveniles.[7,8] The main mode of transmission for FECV is fecal-oral but transmission can occur via direct contact (saliva, grooming behavior), respiratory droplets, and maternal shedding.[1,8,11,17,18] Meanwhile, FIPV infects and replicates in monocytes/macrophages and is associated with a severe, multisystemic immunoinflammatory disease.[1,7,8,11,13] The amount of replicating virus shed in FIPV-positive cats is extremely low with diminished replication in the enterocytes, therefore capacity for horizontal transmission is unlikely.[8,14] Feline infectious peritonitis (FIP) is an invariably fatal disease of both domestic and wild felids.[1,6-8,11-13,15,16] Outbreaks are related to environmental (crowding, concurrent infections, long-term exposure to shedders), virus, and host (individual immune response) factors.[8,13]The prevailing thought is that FIPV results from a mutated feline enteric coronavirus (in vivo mutation transition/internal mutation theory). [1,6-8,10-18] A single mutation has not been identified, rather multiple mutations associated with the 3C accessory gene and fusion and binding domains of the spike (S) protein are common in virulent biotypes.[1,7,8,11,13,14,17] Significant mutations in the FECV genome facilitates switching to FIPV by imparting tropism for macrophages, as well as productive and sustained replication in macrophages.[1,6-8,10-18] Acquired virulence factors allow for dissemination via leukocyte trafficking.[1,7,8,12-14,17] An alternative, less prominent theory states that FIP infections are due to distinct circulating avirulent and virulent strains, which may be the case in rare outbreaks.[8,14,16] FIP typically occurs in young or geriatric cats, with multi-cat environments, stress, and immunosuppression known risk factors.[7, 8,11,12,16] Increased incidence is reported in Abyssinians, Bengals, Birmans, Himalayans, Ragdolls, and Rex breeds.[7,8,11]

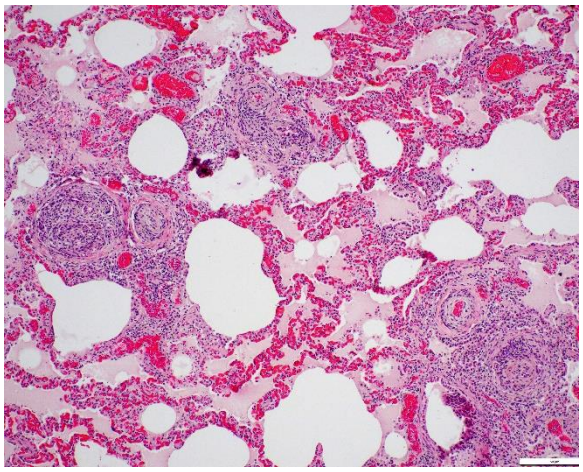

Figure 4-4. Lung, cat. Vascular lumens are commonly filled by plexiform lesions characterized by sieve-like masses comprised of a core of an extracellular matrix, smooth muscle cells, and stromal cells lined by quiescent and hypertrophied endothelial cells (HE, 100X) (*Photo courtesy of:* Schwarzman Animal Medical Center,http://www.amcny.org/)

Individual immune-responses play an essential role in FIPV disease progression.[7,8,13,14] Protective immunity is considered cell-mediated.[8,14] Severe disease is linked to a strong humeral response that is ineffective in virus elimination and simultaneous weak cell-mediated response.[1,7,8,11-14,17] Depletion and reduced cytotoxicity of NK cells coupled with decreased regulatory T-cells (Tregs) are seen in FIP cats.[8,14] In FIP infections a robust antibody response increases the severity of the disease, a phenomenon known as antibody dependent enhancement. [7,8,12-14,17,18] Classic FIP manifestations are "wet"/effusive and "dry"/pyogranulomatous forms, but a combination of the two is common.[1,7,8,11-14,16] The individual animal's immune response is thought to direct the spectrum of pathology.[1,7,8,11-14,16] With a vigorous cell-mediated response FIP lesions do not develop, while in patients who lack a cell-mediated response and have a strong humoral response the "wet"/effusion form develops.[1,8,12-14,17] The "dry"/pyogranulomatous form is associated with an intermediate response. [1,7,8,14,17] Typical gross pathology seen in the "wet" form is a fibrinous polyserositis with a viscous, high-protein, yellow exudative effusion with variable parenchymal involvement.[1,7,8,11,12, 14,16,17] With the "dry" form distinct granulomas/pyogranulomas throughout the body cavities and viscera are seen, which classically track along blood vessels and are not accompanied by effusion.[1,7,8,11,12,14,16,17] Commonly affected organs include the omentum, serosa, peritoneum, kidney, brain, and eye.[7,8,18] With brain involvement, meningeal plaques, intraventricular protein and fibrin-rich exudate, hydrocephalus, and cerebellar herniation can be seen. [7,12] Ocular manifestations include conjunctivitis, high-protein fluid in the anterior and posterior chambers, keratic precipitates, and retinal detachment.[7,10] Microscopic changes include characteristic vasculocentric, pyogranulomatous to pleocellular inflammation with overt phlebitis and variable vascular necrosis that preferentially involves small to medium size veins.[1,7,8,11,12,14,16,17] A similar progressive multisystemic inflammatory disease has been described in ferrets with coronavirus infection, which has been denoted as ferret systemic coronavirus.[6,7,11,12,15, 18]

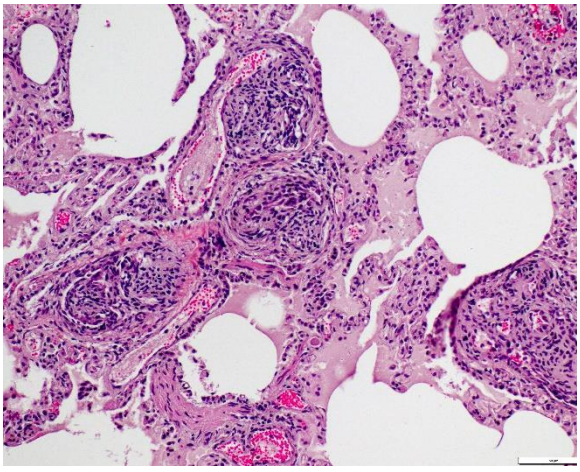

Figure 4-5. Lung, cat. Higher magnification of plexiform lesions. (HE, 400X) (*Photo courtesy of:* Schwarzman Animal Medical Center, http://www.amcny.org/)

Activation of FIP viral-infected macrophages contribute to the characteristic histopathologic changes, perivascular lesion distribution, and vascular damage with resulting vascular leakage.[7,8,11,16,17] Activated tissue macrophages secrete proinflammatory cytokines (TNFα, IL1β, IL6, IFNγ, GM-CSF and G-CSF), matrix enzymes (MMP9), and leukocyte adhesion molecules, as well as upregulation of surface integrins (CD18, CD11a, and CD49d) that lead to leukocyte chemotaxis, induce differentiation and proliferation of additional monocytes and neutrophils, intensify the inflammatory reaction, increase vascular permeability, and exacerbate tissue damage.[7, 8,11,13,14,16,17] Compliment activation accelerates chemotaxis and leukocyte adhesion.[16,17] Increased VEGF transcription and levels in infected cats further increase vascular permiability.[8,14] Both immune-mediated type III and type IV hypersensitivity reactions are hypothesized to play a role in the vascular lesions and perivascular inflammation.[7, 14] Antigen-antibody immune complexes and antibody-complement complexes deposit in vessel walls and perivascular tissues where they initiate tissue damage and recruit inflammatory cells.[7,8,12-14,16,17] Hyperstimulation of T-cells and macrophages, via type IV delayed hypersensitivity, cause perivascular tissues.[7,12,17]

Clinical signs associated with FIPV tend to be vague, non-specific, and depends on varying organ involvement.[1,7,11,12,16] FECV and FIPV cannot be distinguished serologically or morphologically making antemortem diagnosis of FIP challenging and therefore clinical signs and antemortem diagnostics need to be evaluated in concert using a diagnostic algorithm.[8,14] Bloodwork changes associated with FIP include lymphopenia, regenerative anemia, hypoproteinemia due to hypergammaglobulinemia, and biochemical changes associated with specific organ involvement.[8] FIP

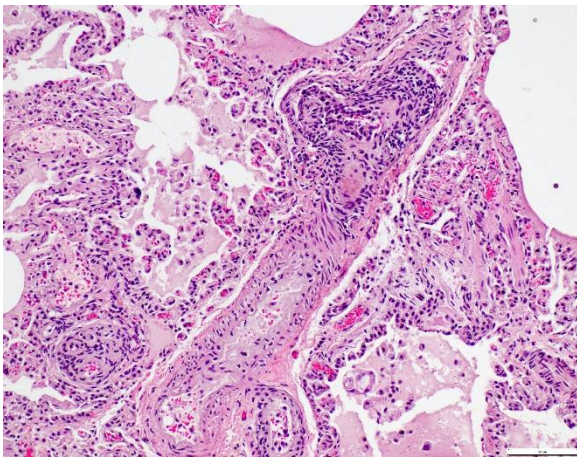

Figure 4-6. Lung, cat. When longitudinally sectioned, plexiform lesions are prominent at branch points. (HE,400X) (*Photo courtesy of:* Schwarzman Animal Medical Center, http://www.amcny.org/)

effusions typically have a high protein content (> 35g/L) with concurrent low cellularity (< 3500 nucleated cells/ml).[8] A serum albumin: globulin (A:G) ratio <0.8 is highly suggestive of FIP infection; meanwhile, an effusion A:G ratio <0.4 has a high positive predictive value for FIP.[8] Acute phase proteins, including alpha1 acid glycoprotein (AGP), are elevated with FIP.[8] Higher titers (≥1:1600) for FCoV-specific antibodies in the blood and effusion are more indicative of FIP.[8] RT-PCR can detect virus in feces, blood, and effusions but cannot differentiate between the two biotypes.[8] Immunohistochemistry allows for confirmation of coronavirus antigen within lesions on biopsy or postmortem samples, as in this case.[11]

The prominent vascular changes in this patient are characteristic for plexogenic pulmonary arteriopathy, a set of morphologic changes associated with pulmonary arterial hypertension (PAH). Causes of pulmonary hypertension include idiopathic (primary) PAH, systemic-to-pulmonary vascular shunts (including patent ductus arteriosus), chronic pulmonary thromboembolic disease, disor-

ders of pulmonary blood vessels (e.g., heartworm disease, pulmonary veno-occlusive disease, pulmonary vasculitis), hypoxic vasoconstriction, chronic interstitial lung disease, or pulmonary venous hypertension due to left-sided heart failure.[3] In the submitted case, PAH-associated lesions were associated with a known risk factor or condition (i.e., reported PDA).[3,19] Altered vascular tone is believed to be the result of imbalanced vasodilatory (e.g., prostacyclin, NO and cGMP) and vasoconstricting (e.g., endothelin, thromboxane A2, and serotonin) molecules.[3] Other implicated vasoactive molecules include TGFβ, BMP-2, FGF, and platelet-derived growth factor.[3] PAH results in endothelial injury/degeneration, vasculitis, fibrinoid vascular necrosis, smooth muscle proliferation, and "onion skin" perivascular fibrosis.[3,5,19] Thus, the vascular remodeling seen with PAH is considered the result rather than cause of hypertension; however, narrowed vascular lumens can exacerbate pulmonary hypertension.[3,5,19] Right ventricular pressure overload secondary to increased vascular resistance leads to right ventricular eccentric hypertrophy and ultimately right-sided congestive heart failure.[2,19]

PAH-associated histopathology represents a spectrum of both constrictive (medial and intimal remodeling) and complex (plexiform and dilative); these include endothelial hypertrophy, intimal, medial, and adventitial fibrosis, muscularization of small arterioles, vasculitis, thrombosis, plexiform lesions, and adventitial edema.[2-4,19] In humans, lesions are separated into grade I (muscular hypertrophy), grade 2 (intimal proliferation), grade 3 (concentric laminar intimal fibrosis), grade 4 (necrotizing vasculitis), grade 5 (plexiform lesions), and grade 6 (dilation and angiomatoid lesions) changes.[4] Higher grade lesions are typically associated with higher pulmonary artery pressures, although they do not represent a sequential disease progression

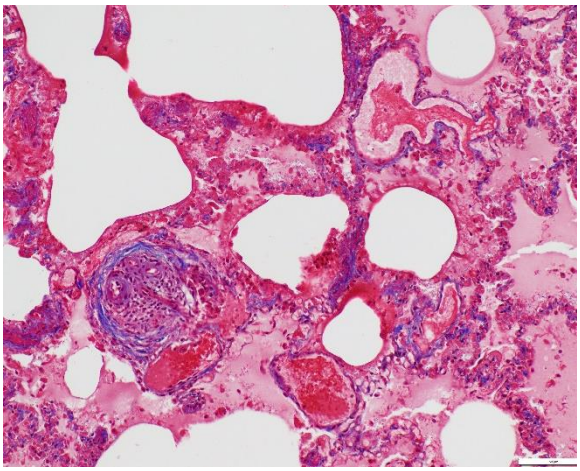

Figure 4-7. Lung, cat. Multiple blood vessels are moderately to severely distended by sac-like dilations (highlighted by Masson's trichrome stain) (Masson's trichrome, 400X) (*Photo courtesy of:* Schwarzman Animal Medical Center, http://www.amcny.org/)

and all grades can develop independently or concurrently.[4, 19] As in this case, characteristic plexiform lesions are characterized by vascular lumens filled by web-like proliferations formed by a core of smooth muscle cells and/or collagenous stroma lined by endothelial cells, which eventually lead to irreversible obliteration of the arterial lumens.[2-5,19] Lesion distribution is to the small muscular arteries and arterioles particularly at the branching points.[2-5,19] Dilation and angiomatoid lesions tend to occur at the artery/arteriole distal to the lesion suggesting impaired blood flow in their development.[2-5] Secondary pulmonary hemorrhages can be seen.[4] Plexiform lesions are dynamic structures involving the cross-talk between quiescent endothelial cells, apoptosis-resistant myofibroblasts, smooth muscle cells, and undifferentiated cells at the lesion's core.[2,5] Jet lesions at mouth of branch vessel and necrotizing arteritis may contribute to lesions.[5] Plexiform lesions are thought to be chronic attempts to repair injured vessels and likely represent cellular, recanalized thrombi secondary to vascular damage.[3-5]

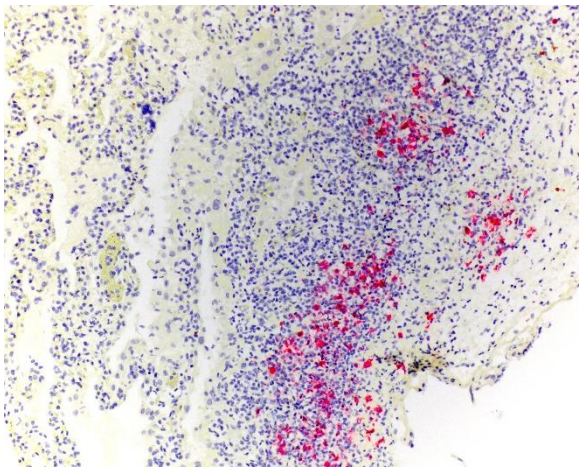

Figure 4-8. Lung, cat. Macrophages within the pleural granulomas stain strongly for feline coronavirus antigen. (anti-FIPV,400X) (*Photo courtesy of:* Schwarzman Animal Medical Center, http://www.amcny.org/)

Contributing Institution:
Schwarzman Animal Medical Center
510 E. 62nd Street
New York, NY 10065
http://www.amcny.org/

JPC Diagnosis:
1. Lung: Pneumonia, interstitial, lymphohistiocytic and neutrophilic, chronic, diffuse, moderate, with multifocal fibrinonecrotizing pleuritis.
2. Lung, small arterioles: Plexiform (plexogenic) arteriopathy, chronic, multifocal, severe with marked intimal hyperplasia and medial hypertrophy, fibrinoid necrosis, thrombosis, and recanalization.

JPC Comment:
The final case of this conference is quite complex with a plethora of features to put together to arrive at a final understanding of the case. Conference participants did not have access to the gross photos from this case (figures 4-1 and 4-2) beforehand, though they are highly suggestive of FIP and assist with interpretation of microscopic changes. The interstitial pneumonia and pleuritis are expected microscopic correlates (figures 4-3 and 4-4), though the vascular features are initially puzzling as the pulmonary veins lack overt phlebitis in the sections available while smaller pulmonary arteries have features reflecting hypertension (figures 4-5 and 4-6) which is not associated with FIP. Conference participants struggled to nail down how to best capture this feature as the arterial response to hypertension (plexiform) is not as commonly described perivascular concentric lamellated fibrosis ('onion skin'). Readers that are interested in exploring the genesis of this lesion in detail would greatly benefit from reviewing the excellent summary by Carman et al.[2]

Briefly, plexiform-type vascular changes arise from nonspecific medial and adventitial thickening of the pulmonary artery with extension of smooth muscle to small non-muscular arteries.[2] Subsequent complex remodeling driven by dysfunctional,[5] hyperproliferative, and apoptosis-resistant pulmonary endothelial cells leads to aberrant signaling between smooth muscle cells and fibroblasts with the result being progressive obliteration of the lumen of the vessel by laminar, stalk-like, or complete aneurysm-like projections of endothelial cells overlying a core of smooth muscle and/or collagenous stroma.[2] HIF-2α and VEGF signaling likely play a role and models of disease have focused on hypoxia as an inciting event in the development of this lesion though other concurrent factors are likely needed to induced complex lesions.[2,5] Interestingly, animals with experimentally treated with inhibition of VEGFR and hypoxic conditions that were later returned to normoxia developed large-scale plexiform pulmonary lesions. The interplay of ineffective endothelial apoptosis, strong impetus for angiogenesis, and aberrant cytokines and growth factors derived from a 'misguided' endothelial cell ringleader[5] is a solid hypothesis though this phenomenon remains incompletely understood.

References:

1. Andre NM, Miller AD, and Whittaker. Feline infectious peritonitis virus-associated rhinitis in a cat. *Journal of Feline Medicine and Surgery Open Reports*. 2020; 1-6.
2. Carman BL, Predescu DN, Machado R, et al. Plexiform Arteriopathy in Rodent Models of Pulmonary Arterial Hypertension. *The American Journal of Pathology*. 2019; 189(6): 1133-1144.
3. Caswell JL and Williams KJ. Respiratory System. In: Maxie MG, ed. *Jubb, Kennedy and Palmer's Pathology of Domestic Animals*. Vol 2. 6th ed. Philadelphia, PA: Elsevier Saunders; 2016: 492.
4. Churg A and Wright JL. Pulmonary Hypertension. In: Leslie KO and Wick MR, eds. *Practical Pulmonary Pathology*. 3rd ed. Philadelphia, PA: Elsevier; 2018: 404-407.
5. Fishman AP. Changing Concepts of the Pulmonary Plexiform Lesion. *Physiol Res*. 2000; 49: 485-492.
6. Garner MM, Ramsell K, Morera N, et al. Clinicopathologic Features of a Systemic Coronavirus-Associated Disease Resembling Feline Infectious Peritonitis in the Domestic Ferret (*Mustela putorius*). *Vet Pathol*. 2008; 45: 236-246.
7. Haake C, Cook S, Pusterla N, et al. Coronavirus Infectious in Companion Animal: Virology, Epidemiology, Clinical and Pathologic Features. *Viruses*. 2020; 12:1023-1043.
8. Kipar A and Meli ML. Feline Infectious Peritonitis: Still an Enigma? *Veterinary Pathology*. 2014; 51(2): 505-526.
9. Koharto A, Toba M, Alzoubi A, et al. Formation of Plexiform Lesions in Experimental Severe Pulmonary Arterial Hypertension. *Circulation*. 2010; 121: 2747-2754.
10. Labelle P. The Eye. In: Zachary JF and McGavin MD, eds. *Pathologic Basis of Veterinary Disease*. 7th eds. St Louis, MO: Elsevier. 2022; 1432.
11. Maclachlan NJ and Dubovi EJ. Coronavirus. In: Maclachlan NJ and Dubovi EJ, eds. *Frenner's Veterinary Virology*. 5th eds. Elsevier. 2017: 435-449.
12. Miller AD and Porter BF. Nervous System. In: Zachary JF and McGavin MD, eds. *Pathologic Basis of Veterinary Disease*. 7th eds. St Louis, MO: Elsevier. 2022; 982-983.
13. Palttrinieri S, Giordano A, Stranieri A, et al. Feline infectious peritonitis (FIP) and coronavirus disease 19 (COVID-19): Are they similar? *Transbound Emerg Dis*. 2021; 68: 1786-1799.
14. Pedersen NC. An update on feline infectious peritonitis: Virology and immunopathogenesis. *The Veterinary Journal*. 2014; 201: 123-132.
15. Shigemoto J, Muraoka Y, Wise AG, et al. Two cases of systemic coronavirus-associated disease resembling feline infectious peritonitis in domestic ferrets in Japan. *Journal of Exotic Pet Medicine*. 2014; 23: 196-200.
16. Spagnoli ST and Gelberg HB. Alimentary System and the Peritoneum, Omentum, Mesentery, and Peritoneal. In: Zachary JF and McGavin MD, eds. *Pathologic Basis of Veterinary Disease*. 7th eds. St Louis, MO: Elsevier. 2022; 485.
17. Stanton JB and Zachary JF. Mechanisms of Microbial Infections. In: Zachary JF and McGavin MD, eds. *Pathologic Basis of Veterinary Disease*. 7th eds. St Louis, MO: Elsevier. 2022; 263-264.
18. Sula MJM and Lane LV. The Urinary System. In: Zachary JF and McGavin MD, eds. *Pathologic Basis of Veterinary Disease*. 7th eds. St Louis, MO: Elsevier. 2022; 755-756.
19. Zabka TS, Campbell FE, and Wilson DW. Pulmonary Arteriopathy and Idiopathic Pulmonary Arterial Hypertension. *Vet Pathol*. 2006; 43: 510-522.